Ground State of the Quasi-1D Compound $BaVS_3$ Resolved by Resonant Magnetic X-Ray Scattering

Ph. Leininger,[1,*] V. Ilakovac,[2,3] Y. Joly,[4] E. Schierle,[5] E. Weschke,[5] O. Bunau,[4] H. Berger,[6] J.-P. Pouget,[7] and P. Foury-Leylekian[7]

[1]*Max-Planck-Institut für Festkörperforschung, Heisenbergstraße 1, D-70569 Stuttgart, Germany*
[2]*LCP-MR, Université Pierre et Marie Curie, CNRS-UMR 7614, F-75231 Paris, France*
[3]*Université Cergy-Pontoise, F-95031 Cergy-Pontoise, France*
[4]*Institut Néel, CNRS-UJF, BP 166, 38042 Grenoble Cedex 9, France*
[5]*Helmholtz-Zentrum Berlin, Albert-Einstein-Straße 15, 12489 Berlin, Germany*
[6]*Institut de Physique de la Matière Complexe, EPFL, 1015 Lausanne, Switzerland*
[7]*Laboratoire de Physique des Solides, Univ. Paris-Sud, CNRS, UMR 8502, F-91405 Orsay Cedex, France*

(Received 17 February 2011; published 21 April 2011)

Resonant magnetic x-ray scattering near the vanadium $L_{2,3}$-absorption edges has been used to investigate the low temperature magnetic structure of high quality $BaVS_3$ single crystals. Below $T_N = 31$ K, the strong resonance revealed a triple-incommensurate magnetic ordering at the wave vector $(0.226\ 0.226\ \xi)$ in hexagonal notation, with $\xi = 0.033$. The azimuthal-angle dependence of the scattering signal and time-dependent density functional theory simulations indicate an antiferromagnetic order within the ab plane with the spins polarized along a in the monoclinic structure.

DOI: 10.1103/PhysRevLett.106.167203 PACS numbers: 75.25.−j, 71.27.+a, 73.63.−b, 75.50.−y

$BaVS_3$ and related compounds have attracted considerable scientific interest in the past decades, mainly due to the interaction between itinerant and localized electrons which involves a subtle interplay between charge, orbital, and spin degrees of freedom [1]. This interplay is responsible for the very rich phase diagram, with a metal-insulator (MI) transition at $T_{MI} = 69$ K and another transition around $T_X = 30$ K. The complex electronic structure and the simple quasi-1D geometry make $BaVS_3$ a model compound for the study of ordering parameters competition.

Much experimental and theoretical work has been devoted to investigate the ground state of $BaVS_3$. However, as most of the research has been done on powder samples, information about the low temperature structure is limited and the results are still contradictory. Nuclear magnetic resonance and nuclear quadrupole resonance measurements revealed a nonmagnetic ground state below T_X and interpreted the asymmetric field gradient at the V sites as a consequence of orbital ordering [2]. Susceptibility measurements also indicated a spin pairing ground state below T_X [3], while heat capacity measurements did not detect any transition [4]. The development of an orbital ordering between T_{MI} and T_X has also been suggested from dielectric function measurements [5]. On the other hand, powder neutron diffraction revealed very few magnetic Bragg peaks sustaining a magnetic ground state [6]. Supposing a ferromagnetic (FM) coupling along c, the structure refinement suggested an incommensurate long-range ordering with the wave vector $(0.226\ 0.226\ 0)_H$ (hexagonal lattice coordinates) in reciprocal lattice units (rlu). A magnetic origin of this transition has also been supposed to explain muon spin resonance measurements [7]. Therefore, the precise nature of the low temperature structure needs to be clarified.

In order to determine the exact nature of the low temperature structure, we used soft resonant magnetic x-ray scattering (RMXS), which has proved to be an excellent tool for probing magnetic ordering in $3d$ materials [8–11]. The large resonant enhancement of the scattering cross section, in combination with the high brilliance of the x-ray beam provided by third generation synchrotron facilities, enable the investigation of small single crystals.

In this Letter we report the direct observation of an antiferromagnetic (AFM) ground state, by RMXS at the V-L edge. Below $T_N = 31$ K, the strong resonance clearly shows an in-plane modulation, which agrees with a previous suggestion, and brings to light a small incommensurate component in the c direction. The simulation of the azimuthal-angle dependence with a time-dependent density functional theory (TD DFT) shows that the spins are polarized along the a direction in the monoclinic structure and allows us to determine the in-plane magnetic structure.

At room temperature the $S = 1/2$ $BaVS_3$ ($3d^1$) system is metallic and its $P6_3/mmc$ structure consists of a hexagonal packing of quasi-1D chains of face-sharing VS_6 octahedra along c, with two V atoms per unit cell (uc) [12]. A zigzag deformation of the V-S chains at 240 K doubles the number of (in-phase) chains in the uc and reduces the crystal symmetry to an orthorhombic structure ($Cmc2_1$) (H-O transition). This transition is accompanied by the creation of 6 twin domains in the ab plane [13]. Peierls instability drives the system to an insulating phase at T_{MI}, lowering further the symmetry to the Im space group [14].

The $2k_F$ charge density wave (CDW) is accompanied by a tetramerization of the V chains. At T_{MI} the magnetic susceptibility shows an AFM-like drop, indicating that the spin degrees of freedom are strongly affected by the MI transition [3,15]. On the other hand, the critical wave vector $2k_F = 0.5c^\star$ ($c^\star$ stands for the reciprocal lattice vector related to c) indicates that only one of the two d electrons per unit cell participates directly in the CDW [14]. The effective moment deduced from the Curie-Weiss behavior of the magnetic susceptibility is $1.223\mu_B$, consistent with one localized spin every other V site [14]. Band structure calculations reveal two different t_{2g} active electron states at the Fermi level [16–18]: two narrow E_g bands and one dispersive A_{1g} band extending along c undergoing the CDW instability [14].

In order to determine the nature of the ground state in $BaVS_3$, we investigate the reflection at (0.226 0.226 ξ). First, we measure the energy dependence of the scattered signal to show its resonant character. From the temperature and azimuthal-angle dependence, we determine the magnetic origin of the signal as well as the incommensurability along c. The simulation of the azimuthal-angle dependence with TD-DFT calculations is used to determine the in-plane magnetic structure.

The experiments were performed at the UE46-PGM1 beam line at the BESSY II synchrotron light source in Berlin, using a two-circle diffractometer with horizontal scattering geometry. The sample was mounted on a copper goniometer and attached to a continuous He-flow cryostat cooling the sample down to 10 K. The signal was recorded with a photodiode with a vertical (horizontal) acceptance of 4° (0.4°) providing a momentum resolution of 0.001 rlu. The $BaVS_3$ single crystal, grown as explained elsewhere [19], with a size of $2 \times 3 \times 0.5$ mm^3, was aligned along $[110]_H$, allowing a rotation about the scattering vector. The results shown here are mainly obtained on an uncleaved surface and subsequently confirmed on an *in situ* cleaved surface.

At 10 K, a strong resonant enhancement of the scattered intensity is observed at the wave vector $(0.226 \pm 0.001\ 0.226 \pm 0.001\ \xi)_H$ near the V-$L_{2,3}$ absorption edges (Fig. 1), indicating that the signal is related to the $3d$ electrons. This result is the first direct observation on a single crystal of the in-plane components of the magnetic ordering vector suggested from powder neutron diffraction [6]. The x-ray absorption spectra (inset of Fig. 1) show two main structures with maxima at 517 and 524 eV, corresponding, respectively, to the V-L_3 ($2p_{3/2} \rightarrow 3d$) and V-L_2 ($2p_{1/2} \rightarrow 3d$) dipole transitions. The resonant signal presents two double peak structures near 515 and 523 eV close to the V-L_3 and L_2 absorption edge, respectively (Fig. 1). It can be attributed to different t_{2g} states and related to two temperature dependent structures observed by total electron yield measurement [20]. The scattered intensity disappears at $T_N = 31 \pm 1$ K (see inset of Fig. 2) at the same transition temperature reported in previous experiments [3,6,7].

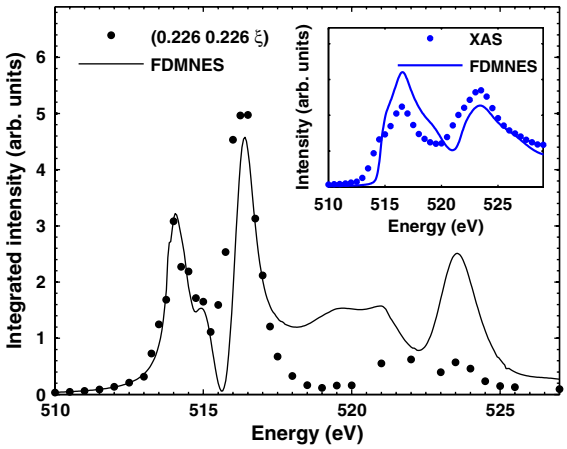

FIG. 1 (color online). Energy dependence of the magnetic reflection at (0.226 0.226 ξ) measured at 10 K. The solid line is the result of the FDMNES code calculation (see text). The inset shows the V-$L_{2,3}$ x-ray absorption spectra (XAS) recorded in total fluorescence yield mode (dots) and compared with FDMNES simulation (solid line).

To determine precisely ξ, the rocking curve of the magnetic signal was measured at two different azimuthal angles, $\Psi = 0°$ and $\Psi = 90°$ (Fig. 2). The scattering geometry and the definition of Ψ are illustrated in Fig. 3. Note that at $\Psi = 0°$ (90°) a and b (c) are in the scattering plane. At $\Psi = 0°$ several structures related to different

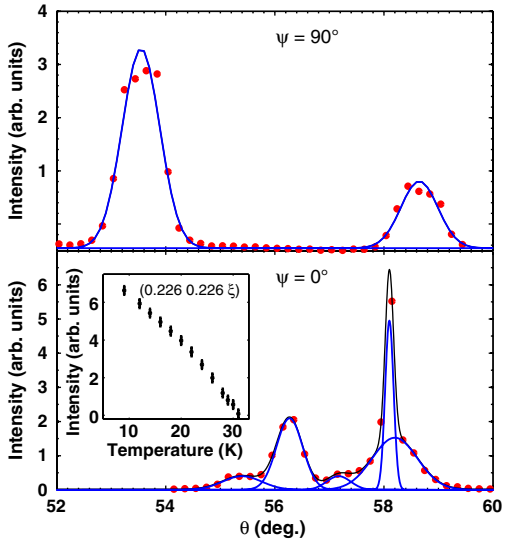

FIG. 2 (color online). Rocking curve of the magnetic signal measured at $\Psi = 90°$ (upper panel) and at $\Psi = 0°$ (lower panel). The gray (blue) lines correspond to a fit with a Gaussian profile. The inset shows the temperature dependence of the (0.226 0.226 0.033) magnetic reflection measured at 10 K with 516.5 eV photon energy.

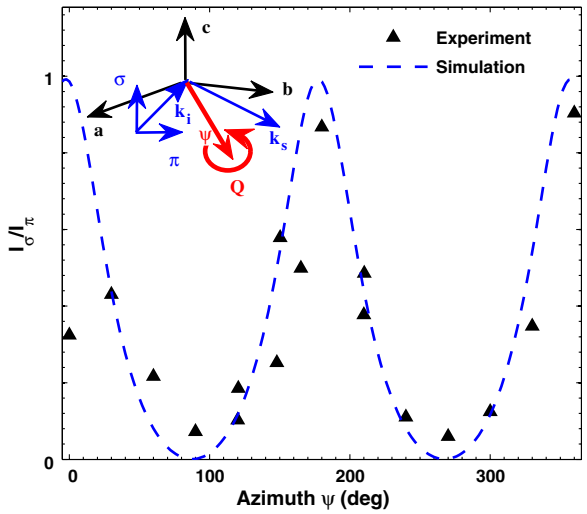

FIG. 3 (color online). Azimuthal-angle (Ψ) dependence of the ratio of resonant-peak intensities measured with σ and π incident polarized beam (black triangles). The blue dashed line corresponds to the FDMNES simulation when the spins are polarized along a_{Im} (see text). The schematic illustrates the definition of Ψ and shows the scattering geometry at $\Psi = 0°$.

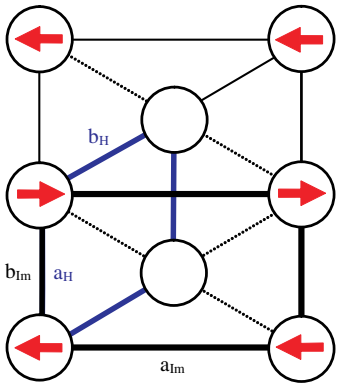

FIG. 4 (color online). Magnetic structure of $BaVS_3$ in the monoclinic (black) and hexagonal [gray (blue)] lattice deduced from combined RMXS measurements and *ab initio* calculations.

twin domains are clearly observed, while at $\Psi = 90°$ the rocking curve shows only two well-separated peaks. These two peaks, separated by $\Delta\theta = 4.77°$, are a fingerprint of two incommensurate magnetic reflections at $(0.266\ 0.226\ \pm \xi)$. When $\Psi = 90°$ the magnetic signal from different twin domains is integrated vertically and cannot explain the two structures. $\Delta\theta$ is therefore a parameter able to determine accurately the incommensurability along c^*, with a calculated value $\xi = 0.033 \pm 0.001$ in rlu [21]. Its small value indicates that the interactions are mainly FM, in agreement with previous predictions.

In order to determine the spin polarization, the magnetic signal over a complete azimuthal period has been measured on one twin domain. To avoid surface and sample size effects, Fig. 3 shows the ratio I_σ/I_π, where I_σ and I_π are the intensities recorded with incoming polarization, respectively, perpendicular and parallel to the scattering plane. The spectra have a period π with a maximum at $\Psi = 180°$ and a minimum at $\Psi = 90°$. Because of the complexity of the structure and the multielectronic phenomena occurring in the resonant scattering process, we used simulations to determine the best magnetic structure compatible with the experiments.

Simulations were performed with the FDMNES code [22]. It has already been extensively used to simulate resonant elastic scattering spectra in a large variety of compounds, mainly at K edges. To take into account the strong photoelectron-hole interaction occurring at the $L_{2,3}$ edges of transition metals, time-dependent density functional theory was recently incorporated in the code [23]. It was first developed by Runge and Gross [24] and later applied to simulate x-ray absorption spectra in $3d$ transition metal compounds [25]. We present here its first use in the context of RMXS. Calculations are fully relativistic and use a local exchange correlation kernel including the spin-orbit coupling for both the core and valence states without any approximation. To calculate the resonant atomic scattering amplitude, we use the multiple scattering frame in 5 Å radius clusters around each absorbing atom containing around 23 atoms.

Starting from the low temperature I_m monoclinic cell based on the crystal structure of Fagot *et al.* [13], several magnetic models have been considered. The simulations were done in the simplest $1 \times 2 \times 1$ monoclinic supercell, with the spins polarized in the ab plane and an AFM coupling along b_{Im} (Fig. 4). In this supercell 4 layers of V atoms contain 8 inequivalent V. One layer is schematically represented in Fig. 4, where the 2 nonmagnetic V atoms are located at the nodes of the spin wave. No spin frustration takes place and one spin $S = 1/2$ every two V atoms in the uc is in agreement with Refs. [13,14,26]. The calculations are done with the $(0, -1/2, 0)_{Im}$ magnetic reflection equivalent to $(h', -2h', 0)_H$, with $h' = 0.25$. Because of the sixfold symmetry of the hexagonal structure this reflection is experimentally indistinguishable from the $(h', h', 0)_H$. The calculated x-ray-absorption spectroscopy and resonant scattering spectra reproduce the overall shape of the experimental data (Fig. 1), and the excellent agreement of the peak positions indicates the correct treatment of the multielectronic effects.

Simulations on a larger supercell, like the $1 \times 20 \times 1$ with a $20b_{Im}/9$ modulation ($h' = 0.225$ very close to $h = 0.226$, the experimental indexation), does not change the results of the calculation. Adding a magnetic moment on the central V atoms does not influence the shape of the spectra but introduces a modification in the intensity. The calculation in the $4 \times 4 \times 1$ supercell, corresponding to the $(h', h', 0)_H$ reflection, leads to a spin wave along $(110)_H$ and does not affect the simulated azimuthal dependence.

Moreover, this cell is less reliable because the AFM ordering extends along the $a_{Im} + b_{Im}$ direction where the V-V distances are longer.

The best I_σ/I_π simulation (Fig. 3) is obtained with the magnetic structure represented in Fig. 4, where the spins on the V atoms are polarized along a_{Im}. A clear maximum (minimum) is seen at $\Psi = 180°$ ($\Psi = 90°$) in agreement with the experiment. This result is also supported by the susceptibility (χ) measurements which pointed out that below T_N, χ_{ab} is smaller than χ_c, indicating an easy axis within ab [3]. When the spins are polarized along b_{Im} the simulated azimuthal spectra is shifted by a $\pi/2$ phase with respect to the experiment, and with a magnetic moment oriented along c_{Im}, I_σ/I_π is equal to unity.

Usually the RMXS data are analyzed with the standard formula $|(\hat{\epsilon}_i^* \times \hat{\epsilon}_s) \cdot \hat{m}|^2$ [27,28], where $\hat{\epsilon}_i$ ($\hat{\epsilon}_s$) is the polarization of the incoming (scattered) photons and $\hat{m}$ the unit vector of the density of magnetic moment. Nowadays the validity of this simple formula is under debate because of the possible effects of the local symmetry which are not taken into account [27,29]. But due to the orientation along a high symmetry direction of the magnetic moment, it remains valid for the present compound. This validity is confirmed by our more sophisticated TD-DFT calculations.

In summary, the strong resonant enhancement observed below $T_N = 31$ K at the V-$L_{2,3}$ edges at reflection $(0.226\ 0.226\ 0.033)_H$ reveals a triple magnetic incommensurate ordering in $BaVS_3$. The temperature and azimuthal-angle dependence of the signal attest to the magnetic origin of the transition at T_N. Through simulation of the resonance with the FDMNES code in a TD-DFT multiple scattering frame, we reproduced the experimental data and established that the ordering is AFM in plane with the spins polarized along a_{Im}. The long-range modulation along c shows that the interactions are predominantly FM, indicating either a conical structure with the magnetic moment slightly deviated from the a axis or a spin-density wave along c. A neutron diffraction refinement on a bigger sample could determine the full structure in the c direction. Further theoretical investigations are also needed to explain the precise origin of this out-of-plane modulation. We believe that the determination of the magnetic structure in $BaVS_3$ will help ongoing efforts for further theoretical work which may help to understand the puzzling interplay between magnetic, charge, and orbital order in low-dimensional systems.

We are grateful to I. Zegkinoglou, M. W. Haverkort, D. Efremov, G. Jackeli, C. F. Hague, and B. Keimer for discussions and helpful suggestions. We would like to thank C. Schüßler-Langeheine for instrumental support.

*Corresponding author.
pleining@laposte.net

[1] M. Imada, A. Fujimori, and Y. Tokura, Rev. Mod. Phys. **70**, 1039 (1998).
[2] H. Nakamura, H. Imai, and M. Shiga, Phys. Rev. Lett. **79**, 3779 (1997).
[3] G. Mihály *et al.*, Phys. Rev. B **61**, R7831 (2000).
[4] H. Imai, H. Wada, and M. Shiga, J. Phys. Soc. Jpn. **65**, 3460 (1996).
[5] T. Ivek, T. Vuletić, S. Tomić, A. Akrap, H. Berger, and L. Forró, Phys. Rev. B **78**, 035110 (2008).
[6] H. Nakamura *et al.*, J. Phys. Soc. Jpn. **69**, 2763 (2000).
[7] W. Higemoto *et al.*, J. Phys. Soc. Jpn. **71**, 2361 (2002).
[8] P. Abbamonte, A. Rusydi, S. Smadici, G. D. Gu, G. A. Sawatzky, and D. L. Feng, Nature Phys. **1**, 155 (2005).
[9] J. Schlappa *et al.*, Phys. Rev. Lett. **100**, 026406 (2008).
[10] S. B. Wilkins, P. D. Hatton, M. D. Roper, D. Prabhakaran, and A. T. Boothroyd, Phys. Rev. Lett. **90**, 187201 (2003).
[11] P. Leininger *et al.*, Phys. Rev. B **81**, 085111 (2010).
[12] R. A. Gardner, M. Vlasse, and A. Wold, Acta Crystallogr. Sect. B **25**, 781 (1969).
[13] S. Fagot *et al.*, Solid State Sci. **7**, 718 (2005).
[14] S. Fagot, P. Foury-Leylekian, S. Ravy, J.-P. Pouget, and H. Berger, Phys. Rev. Lett. **90**, 196401 (2003).
[15] M. Takano *et al.*, J. Phys. Soc. Jpn. **43**, 1101 (1977).
[16] L. F. Mattheiss, Solid State Commun. **93**, 791 (1995).
[17] M. H. Whangbo, H. J. Koo, D. Dai, and A. Villesuzanne, J. Solid State Chem. **165**, 345 (2002).
[18] F. Lechermann, S. Biermann, and A. Georges, Phys. Rev. B **76**, 085101 (2007).
[19] H. Kuriyaki, H. Berger, S. Nishioka, H. Kawakami, K. Hirakawa, and F. A. Lévy, Synth. Met. **71**, 2049 (1995).
[20] V. Ilakovac *et al.* (unpublished).
[21] H. Nakamura (private communication).
[22] Y. Joly, Phys. Rev. B **63**, 125120 (2001).
[23] O. Bunau and Y. Joly (to be published).
[24] E. Runge and E. K. U. Gross, Phys. Rev. Lett. **52**, 997 (1984).
[25] J. Schwitalla and H. Ebert, Phys. Rev. Lett. **80**, 4586 (1998).
[26] S. Fagot *et al.*, Phys. Rev. B **73**, 033102 (2006).
[27] J. P. Hannon, G. T. Trammell, M. Blume, and D. Gibbs, Phys. Rev. Lett. **61**, 1245 (1988).
[28] J. P. Hill and D. F. McMorrow, Acta Crystallogr. Sect. A **52**, 236 (1996).
[29] M. W. Haverkort, N. Hollmann, I. P. Krug, and A. Tanaka, Phys. Rev. B **82**, 094403 (2010).